Unimolecular Decomposition of Methyltrichlorosilane: RRKM Calculations

ARTICLE *in* THE JOURNAL OF PHYSICAL CHEMISTRY · JULY 1994

Impact Factor: 2.78 · DOI: 10.1021/j100079a018

3 AUTHORS, INCLUDING:

Mark D Allendorf
Sandia National Laboratories
212 PUBLICATIONS **8,310** CITATIONS

Unimolecular Decomposition of Methyltrichlorosilane: RRKM Calculations

Thomas H. Osterheld, Mark D. Allendorf,* and Carl F. Melius

Combustion Research Facility, Sandia National Laboratories, Livermore, California 94551-0969

Received: May 6, 1993®

On the basis of reaction thermochemistry and estimates of Arrhenius *A* factors, it is expected that Si–C bond cleavage, C–H bond cleavage, and HCl elimination will be the primary channels for the unimolecular decomposition of methyltrichlorosilane. Using RRKM theory, we calculated rate constants for these three reactions. The calculations support the conclusion that these three reactions are the major decomposition pathways. Rate constants for each reaction were calculated in the high-pressure limit (800–1500 K) and in the falloff regime (1300–1500 K) for bath gases of both helium and hydrogen. These calculations thus provide branching fractions as well as decomposition rates. We also calculated bimolecular rate constants for the overall decomposition in the low-pressure limit. Interesting and surprising kinetic behavior of this system and the individual reactions is discussed. The reactivity of this chlorinated organosilane is compared to that of other organosilanes.

Introduction

The high-temperature reaction chemistry of chlorinated organosilanes is of intrinsic interest to the field of organosilicon chemistry. Although the thermochemistry[1,2] and reactions of organosilanes have been studied extensively, particularly with regard to the importance of silylenes,[3-5] comparable investigations of chlorinated organosilicon compounds have not been performed. Methylsilane (CH_3SiH_3) pyrolysis, for example, has been investigated in some detail,[6-9] but we are aware of only one study of the pyrolysis of chloromethylsilanes.[10] Recently, Su and Schlegel have used *ab initio* MO methods to study the thermal decomposition of the related chlorinated monosilanes ($SiH_{4-n}Cl_n$).[11] The reactivity of chlorinated organosilicon compounds differs from simple organosilanes primarily because Si–Cl bonds (in tetravalent compounds) are considerably stronger (111–118 kcal mol^{-1})[12] than either Si–H (90–95 kcal mol^{-1})[1] or Si–C (90–94 kcal mol^{-1})[1] bonds. These strong bonds contribute to higher activation barriers for the elimination/insertion reactions that are so prevalent[6-9] in nonchlorinated organisilicon systems. This limits the (unimolecular) reactivity of the silicon functionality and allows access to reactions involving the alkyl group. For example, we will provide evidence that C–H bond cleavage can contribute to chlorinated organosilane pyrolysis. This reaction is not typically expected to play a role in organosilicon pyrolysis, based on both kinetic and thermochemical arguments.[2,13,14] In addition to the increased importance of the H-loss channel, the Cl functionality lowers the barrier for the 1,2-elimination.[15,16] Statistical kinetic calculations on these systems are invaluable in obtaining a better understanding of their behavior and in attaining predictive models of reactivity and kinetics. This is especially true when little experimental data are available, as is the case for chlorinated organosilanes.

In addition to their fundamental chemical importance, chlorinated organosilanes have widespread industrial applications. They serve, for example, as precursors to polydimethylsiloxanes,[17] which find applications ranging from dielectric media to hydraulic fluids and lubricants. Chlorinated organosilanes are also commonly employed in chemical vapor deposition (CVD) processes used to produce silicon carbide (SiC) coatings, thin films, composites, and powders. Composites based on SiC and manufactured using chlorinated organosilanes are considered some of the most advanced materials of their kind.[18] Currently, a variety of new methods for depositing SiC are under consideration, operating at both atmospheric[19,20] and subatmospheric pressure.[21-23] One of the most common reactants used in these processes is methyltrichlorosilane (CH_3SiCl_3, MTS), which is favored because it is nonpyrophoric and inexpensive. It has been shown that MTS decomposes under typical SiC CVD conditions (atmospheric pressure, deposition temperatures >1400 K), producing HCl, $SiHCl_3$, $SiCl_4$, and CH_4 as well as other silanes and hydrocarbons.[24,25] These decomposition products result from both primary and secondary reaction pathways. Models used to optimize and scale-up new SiC CVD processes require detailed knowledge of the gas-phase chemistry for two important reasons. First, the high activation energies of MTS unimolecular reactions may make them the rate-limiting step in the deposition, particularly for low-temperature processes. Second, the surface reactivity of the various gas-phase product species, as characterized by a reactive sticking coefficient Γ, varies widely. Saturated molecules such as $SiCl_4$ react with[26] $\Gamma \leq 10^{-3}$, while radicals such as SiH_n (n = 0–3) are known to react with much higher efficiency,[27-30] $\Gamma \sim 0.1$–1.0. Thus, in order to accurately predict deposition rates, the concentrations of the various species present in the gas phase must be known. Unfortunately, we are aware of only one report in the literature that discusses the kinetics of the gas-phase decomposition of MTS.[25] That paper has been widely cited but contains no data by which the measurements can be critically evaluated.

Recently, we reported estimates of thermodynamic properties of molecules in the Si–C–Cl–H system, obtained from *ab initio* calculations using the BAC-MP4(SDTQ) method.[12] The structure and energetics of a transition state for the 1,2-elimination of HCl from MTS were also included in that study. These data allow activation energies for several possible MTS decomposition pathways to be estimated (Figure 1). They also provide the thermodynamic basis for the calculations reported here.

$$CH_3SiCl_3 \rightarrow CH_3 + SiCl_3 \quad (1)$$

$$CH_3SiCl_3 \rightarrow CH_2SiCl_3 + H \quad (2)$$

$$CH_3SiCl_3 \rightarrow CH_3SiCl_2 + Cl \quad (3)$$

$$CH_3SiCl_3 \rightarrow H_2C{=}SiCl_2 + HCl \quad (4)$$

$$CH_3SiCl_3 \rightarrow CH_3Cl + SiCl_2 \quad (5)$$

$$CH_3SiCl_3 \rightarrow CH_3SiCl + Cl_2 \quad (6)$$

In this paper, we use statistical theory[13,31-49] to calculate rate

* To whom correspondence should be addressed.

® Abstract published in *Advance ACS Abstracts*, January 1, 1994.

0022-3654/94/2098-6995$04.50/0

constants for the unimolecular decomposition of MTS in bath gases of helium or hydrogen. We report rate constants in the high- and low-pressure limits, as well as the complete pressure dependence, for the primary unimolecular decomposition pathways available to MTS (reactions 1, 2, and 4) at temperatures typical of SiC CVD. The results were obtained through the application of Rice–Ramsperger–Kassel–Marcus (RRKM) theory.[32] For calculations in the falloff regime and low-pressure limit, we used bath gases of hydrogen or helium since typical CVD processes use a hydrogen bath gas and there is interest in using inert bath gases. We also report branching fractions as a function of temperature and pressure. The branching fractions allow us to evaluate the importance of organosilicon species in the reaction mechanism converting MTS to SiC. The rate coefficients obtained are compared with the earlier experimental measurement[25] by Burgess and Lewis (BL) of the decomposition of MTS in hydrogen. The calculated rate constant is considerably slower than the BL rate, which was measured at atmospheric pressure in a flow reactor. We also compare a room temperature calculation of the rate constant for reaction 1 to a recently reported association rate (reverse of reaction 1).[50] Our calculated rate is in good agreement with the experiment. In a concluding section, we discuss the significance of these calculations to the field of organosilicon chemistry as well as their implications for SiC CVD processes.

Theoretical Methods

Thermal reaction rate coefficients were calculated using RRKM transition-state theory. Specifically, RRKM theory is used to calculate the microcanonical reaction rate coefficients, $k(E,J)$, which are the rate coefficients for a particular energy (E) and angular momentum state (J) of a molecule. The $k(E,J)$ are then used to calculate thermal rate coefficients which correspond to those measured experimentally. In the high-pressure limit the thermal rate is obtained by averaging the $k(E,J)$ over Boltzmann equilibrium distributions of energy and angular momentum.[32] At lower pressures (referred to as the falloff regime) the reactant energy and angular momentum distributions are no longer Boltzmann. In this regime, the $k(E,J)$ are incorporated into a master equation which also accounts for collisions and collisional energy transfer.[32] Solution of the master equation provides the thermal rate coefficient. The calculations in this paper were accomplished using the UNIMOL suite of Gilbert, Jordan, and Smith[51] after making minor modifications to the RRKM program. An excellent description of RRKM theory and the methods used in performing a calculation can be found in the recent book by Gilbert and Smith,[32] as well as in many other books and articles.[13,31-49]

Our calculations involve modeling reactions having both loose and tight transition states. A loose transition state arises in a bond cleavage reaction where the two fragments are separated by large distances in the transition state. Reactions 1–3 have loose transition states. Usually the motions of the fragments about axes perpendicular to the breaking bond are relatively unhindered (hence the term loose) and are thus treated as 2-dimensional rotors. These rotors contribute significantly to the entropy of the transition state, giving rise to the large Arrhenius A factors typical of bond cleavage reactions.[13] On the other hand, a tight transition state is encountered whenever a reaction requires significant atom rearrangement, as in isomerization or elimination/insertion reactions. Usually the transition state has some critical structure (hence the term tight), and even if two products are formed, the transition state does not have the two fragments separated by large distances. Reactions 4–6 have tight transition states.

The location of the loose transition state along the reaction coordinate (i.e., on a Morse potential) was determined by canonical variational transition-state theory, which means that the transition state was chosen to be the structure that gives the minimum rate in the high-pressure limit.[32] This method requires knowledge of how molecular parameters such as vibrational frequencies and rotational constants change along the reaction cooridate. We used the Gorin model to account for this.[13,32-35] The Gorin model assumes that the transition state is very "product-like" so that each of the two fragments has the structure and vibrational frequencies of the separated products. The separation between the two fragments that gives the minimum rate is then determined using the proper rotational constants for the external and internal rotors at each separation as well as the potential energy at that position on the reaction coordinate.[13,32-35] The two-dimensional rotors of the separating fragments were treated as either hindered rotors or sinusoidal hindered rotors.[33] Steric hindrance was accounted for by the hard-sphere model of Benson in which the density of states for the two-dimensional internal rotors are scaled by a factor that involves the angle through which the fragment can rotate before a steric interaction occurs.[13,32-35] A steric interaction is assumed to occur when hard spheres having radii corresponding to the van der Waals radii of each atom touch. It should be noted that this treatment does not allow for the gradual transition from a free rotor to a sterically hindered rotor and can thus overestimate the steric hindrance.[33] Rotational constants of external and internal rotors, for all of the transition states as well as the reactant, were obtained using the GEOM program from the UNIMOL suite.[51]

TABLE 1: RRKM Parameters for Methyltrichlorosilane and the HCl Loss Transition State[a]

CH_3SiCl_3			$CH_2SiCl_2\cdots HCl^{\dagger}$		
vibrational frequencies			vibrational frequencies		
2991[b] (2)[c]	805 (2)	235 (2)	3154	830	232
2917	762	228	3071	732	202
1411 (2)	572 (2)	164 (2)	1413	630	196
1270	452		1193	487	53
			1186	465	48
			936	406	
B_{ext}(inact), σ_i	0.05800, 1		B_{ext}(inact), σ_i	0.03204, 1	
B_{ext}(act), σ_i	0.04335, 1		B_{ext}(act), σ_i	0.06406, 1	
B_{int}, σ_i, dim	5.436, 3, 1		critical energy	93.0 kcal/mol	
$\sigma_{sym}/n = 3$	$\sigma_{el} = 1$		$\sigma_{sym}/n = 1$	$\sigma_{el} = 1$	

[a] Frequencies and rotational constants are in units of cm^{-1}. [b] Frequencies from ref 54. [c] Degeneracy of vibration.

Structural features and thermodynamic data for the reactant, tight transition states, and the individual fragments in the simple bond cleavage processes were taken from *ab initio* electronic structure calculations using the BAC-MP4(SDTQ) method.[1,52,53] When possible, vibrational frequencies were obtained from the literature and used in the calculations (MTS, $SiCl_3$, and CH_3).[32,54,55] These frequencies were also compared to the vibrational frequencies from the *ab initio* calculations to account for the systematic overestimation of the calculated frequencies.[56] For this system, the *ab initio* calculations appear to overestimate the vibrational frequencies by about 8%. When no literature frequencies were available, as in the case of the HCl loss transition state and the H loss transition state, *ab initio* frequencies were used after scaling by 8%. Reaction thresholds were also determined by *ab initio* calculations. For the discussion in this paper the reaction threshold refers to the critical energy (E_0) of a reaction, which is the minimum energy required for an isolated molecule to undergo reaction (the enthalpy difference between the reactant and transition state at 0 K).

The nature of collisions between reactant molecules and the bath gas contributes to the pressure dependence of the reaction rate. Unfortunately, few data are available on collisional energy transfer between chlorinated or alkylated silanes and He or H_2. We therefore used the semiempirical biased random walk (BRW) model to estimate parameters for collisional energy transfer into internal modes of the reactant.[57-59]

Parameters for the RRKM calculations are given in Tables 1 and 2. The parameters include vibrational frequencies, rotational

TABLE 2: RRKM Parameters for Si–C and C–H Bond Scission Transition States[a]

$CH_3\cdots SiCl_3^\dagger$			$H\cdots CH_2SiCl_3^\dagger$		
vibrational frequencies			vibrational frequencies		
3162[b] (2)[c]	580	254	3180	601	230
3044	582[d] (2)	176 (2)	3086	574	227
1396 (2)	470		1429	530	165
			796	448	157
			787	236	
B_{ext}(inact), σ_i	0.03329, 1		B_{ext}(inact), σ_i	0.04742, 1	
B_{ext}(act), σ_i	0.04277, 1		B_{ext}(act), σ_i	0.05914, 1	
B_{int}, σ_i, dim	4.884, 3, 1		B_{int}, σ_i, dim	7.268, 3, 1	
B_{int}, σ_i, dim	0.06897,[e] 1, 2		B_{int}, σ_i, dim	0.9506, 1, 2	
B_{int}, σ_i, dim	9.681, 2, 2				
D_e	99.9 kcal/mol		D_e	108.9 kcal/mol	
D_0	95.4 kcal/mol		D_0	100.8 kcal/mol	
β	1.82 Å^{-1}		β	1.86 Å^{-1}	
$\sigma_{sym}/n = 3$	$\sigma_{el} = 4$		$\sigma_{sym}/n = 1$	$\sigma_{el} = 4$	

[a] Frequencies and rotational constants are in units of cm^{-1}. [b] Frequencies for CH_3 from ref 32. [c] Degeneracy of vibration. [d] Frequencies for $SiCl_3$ from ref 55. [e] Average hindrance $\Theta = 48°$.

constants for the external (B_{ext}) and internal (B_{int}) rotors, symmetry and degeneracy factors (σ), critical energies, and in the case of the loose transition states the D_e and β parameters for the Morse potential. The rotational constants in Table 2 are for the 1200–1500 K temperature range which are the temperatures used for most of the falloff calculations. We have used the typical treatment for external rotors, in which the molecule or transition state is approximated as a symmetric top. The rotor around the unique axis is treated as active and able to exchange energy with vibrations, while the degenerate 2-dimensional rotor is treated as inactive or uncoupled from the vibrational modes.[32]

Choosing parameters for the reactant is fairly straightforward, although a question arises over how to deal with the torsional vibration. According to the *ab initio* calculation, this vibration in MTS occurs at 165 cm^{-1}. (The torsion is not observed in the infrared or Raman spectra because of its symmetry.) This degree of freedom is treated as a free internal rotor even though the vibrational frequency is fairly high,[32] because the reactions are modeled at high temperatures where we would expect that a free rotor is more appropriate.

For the loose transition states (reactions 1 and 2), we treated the 2-dimensional rotors as sinusoidal hindered rotors.[33] We also calculated rates without the sinusoidal potential for the 2-dimensional rotors. These rates (in the high-pressure limit) are about 30% faster than those using sinusoidal hindered rotors, but the exact values are not reported in this paper. As indicated earlier, steric hindrance was accounted for by the hard-sphere model of Benson.[13]

At room temperature it is easy to locate the transition state for reaction 1 using the techniques described above. As the temperature is raised, the transition state moves to smaller fragment separations.[32] However, over the "high" temperature range used for our calculations, the transition state is not as easy to locate. A problem arises because the hard-sphere model used to account for steric hindrance causes a discontinuity in the rates for reaction 1 at fragment separations in which the 2-dimensional methyl rotor becomes hindered. The discontinuity is an artifact in the calculation and has been described previously.[32-34] The basic difficulty is that the hindering in the hard-sphere model turns on abruptly and strongly so that for reaction 1 it overestimates the steric hindrance for the methyl rotor.[33] We dealt with this by not allowing the methyl rotor to become sterically hindered. This treatment is similar to that of Jordan, Smith, and Gilbert.[33] It is possible that we should have included some steric interaction for this rotor, but *a priori* we have no criteria for choosing the amount of steric interaction. It should be noted that we did include steric hindrance for the $SiCl_3$ rotor in this transition state. We describe below why we believe our treatment

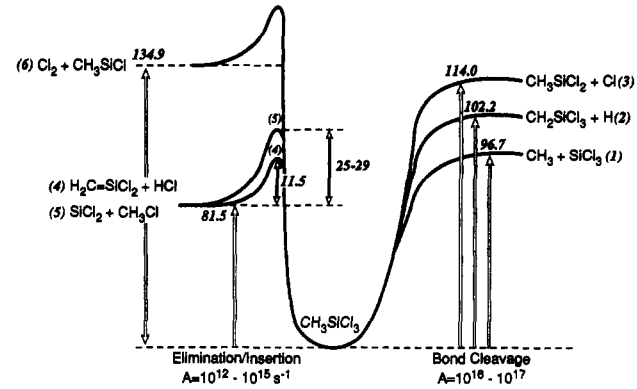

Figure 1. Potential energy diagram showing potential channels for unimolecular decomposition of MTS. Barrier heights and heats of reaction are relative to MTS and are based on thermodyanmic data from ref 12. The values were calculated for 298 K.

is the most appropriate, and then we show by calculations with extreme steric hindrance that our treatment appears correct.

The special treatment of the methyl rotor appears reasonable for several reasons. First, it allows for an unambiguous application of variational transition-state theory. Second, error introduced by failing to hinder the rotor should be at least partially offset by including the symmetry of the rotor ($\sigma = 2$).[60] Including the symmetry results in a lower sum of states than otherwise but would probably not be appropriate if the rotor were significantly hindered. Third, the use of a sinusoidal potential already provides a lower sum of states than the free rotor potential traditionally used in the past. Fourth, when we hindered the methyl rotor, the transition state was located at a position that gave a meaningless rotational constant for the rotor.[32] This indicates that strict use of the hard-sphere model is inappropriate and results in a significant underestimate of the contribution of these modes to the sum of states in the transition state.[32] Finally, test calculations in which we hindered this rotor to any signficant degree actually gave rates *slower* than if the two-dimensional rotor had been treated as two 300–400-cm^{-1} vibrations. Treating the modes as vibrations of this magnitude is an unrealistically tight treatment in our estimation. Since the high-pressure rates calculated in the very hindered extreme of 300–400 cm^{-1} vibrations are only up to a factor of 3 slower than our treatment, we expect that any error introduced from the ambiguity in treating these modes should be minor.

For the H loss transition state (reaction 2), we used the treatment of Benson to obtain rotational constants for the internal 2-dimensional rotor.[13] A reduced moment of inertia is calculated using the moment of the 2-dimensional fragment and the moment of the breaking C–H bond.[61] This treatment accounts for the large mass differences between the two fragments.

The transition state for HCl elimination (reaction 4) has two low-frequency librations. These modes were treated as vibrations and not as a 2-dimensional rotor since an analysis of the hard-sphere steric interactions indicated that a rotor would be completely hindered. This view is supported by a normal-mode analysis of the *ab initio* force field.[62] The reason these two modes have such low frequencies is because they are librations involving a relatively heavy HCl group.

Results

Before discussing the RRKM results, it is useful to review the thermodynamics of the various MTS decomposition pathways, as determined from our previous *ab initio* calculations.[12,52] Figure 1 shows the potential energy curves and reaction enthalpies of several possible MTS decompositions. All of the possible products are considerably higher in energy than MTS (by an amount $\geq$81.5 kcal/mol). In addition, reactions 4 and 5, which are the lowest-energy reactions based on product thermodynamics, have potential energy barriers. This results in a critical energy for any channel

of at least 93.0 kcal/mol. At energies above this, there are five possible reactions in an energy range of about 20 kcal/mol. At much higher energies, reaction 6, which involves breaking strong Si–Cl bonds, also becomes thermodynamically accessible.

We have categorized these reactions as either bond cleavages, having loose transition states with typical Arrhenius A factors[13] of 10^{16}–10^{17} s^{-1}, or elimination/insertion reactions, having tight transition states with typical A factors[13] of 10^{12}–10^{15} s^{-1}. On the basis of these categories and the thermodynamics discussed above, it is a simple matter to remove reactions from consideration that are so slow that they are unlikely to contribute much to the overall decomposition.

Reaction 6, elimination of Cl_2, which has both a low A factor because of a tight transition state and a threshold at least 35 kcal/mol higher than the lowest-energy reaction, can immediately be removed from consideration.

Reaction 3, loss of Cl, which is the highest-energy bond cleavage, can also be eliminated from consideration. We calculated high-pressure A factors using the methods of Benson[13] and found that the A factor for this reaction was similar to those for the other bond cleavages. The much higher threshold (113.4 kcal/mol compared to 95.4 kcal/mol for Si–C bond scission) indicates that it should not contribute significantly to the decomposition.

Finally, reaction 5, elimination of CH_3Cl, can be removed from consideration. Although attempts to calculate this transition state using *ab initio* theory were unsuccessful, we estimate that its threshold will be higher than that for reaction 1 (Si–C bond scission).[52] Since reaction 5 has a much smaller A factor than reaction 1, it is not expected to be significant. This conclusion is borne out by the relatively minor contribution of reaction 4 (the other low-energy elimination reaction) to the overall decomposition (*vide infra*).

We have thus modeled the decomposition of MTS by calculating rates for CH_3 loss, H loss, and HCl elimination (reactions 1, 2, and 4). It is expected that these three reactions are the major contributors to the thermal unimolecular decomposition.

High-Pressure Limit. In the high-pressure limit, collisions with the bath gas are sufficiently rapid that energy and angular momentum have equilibrium Boltzmann distributions.[32] As a consequence, reaction rate coefficients do not depend on the total pressure and are even independent of each other in the case of multichannel reactions. Therefore, the high-pressure unimolecular rate coefficient, k_{uni}^{∞}, is the canonical average of the $k(E,J)$ from RRKM theory and can be calculated without resorting to a master equation.[32] For the bond cleavage reactions (reaction 1 and 2), k_{uni}^{∞} is the rate which is minimized when applying canonical variational transition state theory (the method used in this paper). The high-pressure rate coefficients were calculated at temperatures ranging from 800 to 1500 K for the three reactions of interest. Since these rate constants are for the high-pressure limit, they are, of course, independent of bath gas. The calculated high-pressure rate coefficients and reaction parameters are given in Table 3. As can be seen from these results, CH_3 loss is the most efficient reaction at these temperatures followed by H loss. At 1100 K it is almost 200-fold faster than H loss, but as the temperature is increased, H loss becomes more significant. At 1500 K CH_3 loss has a rate coefficient that is only a factor of 9 larger than H loss. It should also be noted that, according to these calculations, reaction 4 never contributes significantly to the decomposition; over the 800–1500 K temperature range it contributes less than 0.4% to the overall rate coefficient. These calculations are useful for comparing the efficiency of the various channels, especially since they are relatively easy to perform. However, as will be seen below, the high-pressure limit is never achieved in CVD reactors.

Falloff Regime. As the pressure is decreased from the high-pressure limit, collisions between reactant and bath gas are no longer sufficiently rapid to maintain Boltzmann energy and angular momentum distributions.[32] Thus, reaction drains away

TABLE 3: High-Pressure Reaction Rates and Parameters for Methyltrichlorosilane

T (K)	reaction product	k_{uni}^{∞} (s^{-1})	$\log(A^{\infty}/s^{-1})$	E_a^{∞} (kcal/mol)
800	HCl	9.6×10^{-12}	15.1	95.5
	CH_3	5.4×10^{-9}	18.3	97.4
	H	2.8×10^{-11}	17.7	103.6
	total	5.4×10^{-9}		
900	HCl	7.6×10^{-9}	15.1	95.7
	CH_3	4.0×10^{-6}	18.3	97.5
	H	3.9×10^{-8}	17.7	103.7
	total	4.0×10^{-6}		
1000	HCl	1.6×10^{-6}	15.2	96.0
	CH_3	7.8×10^{-4}	18.2	97.5
	H	1.3×10^{-5}	17.8	103.8
	total	7.9×10^{-4}		
1100	HCl	1.3×10^{-4}	15.2	96.3
	CH_3	5.7×10^{-2}	18.1	97.4
	H	1.5×10^{-3}	17.8	103.8
	total	5.9×10^{-2}		
1200	HCl	5.1×10^{-3}	15.3	96.5
	CH_3	2.0	18.0	97.5
	H	7.6×10^{-2}	17.8	103.8
	total	2.1		
1300	HCl	0.12	15.3	96.7
	CH_3	40	18.0	97.5
	H	2.2	17.8	103.8
	total	42		
1400	HCl	1.7	15.4	96.9
	CH_3	510	17.9	97.5
	H	38	17.8	103.8
	total	550		
1500	HCl	17	15.4	97.1
	CH_3	4700	17.9	97.5
	H	460	17.8	103.8
	total	5200		

population from levels above the critical energy (E_0). To obtain the energy distribution and reaction rate coefficient, one must resort to a master equation which also accounts for collisions and collisional energy transfer. In this regime, the thermal reaction rate *does* depend on the total pressure.[32] In a multichannel system the rate of a specific pathway is also influenced by the other reactions. Ultimately, at very low pressures, the reaction reaches the low-pressure limit where conversion of the activated reactant to product is sufficiently faster than collisions that any molecule with $E > E_0$ reacts before it can be deactivated by collisions.[32] At this point the reaction becomes first order in bath gas pressure.[32] The falloff regime connects the high- and low-pressure limits and is the region where neither collisional energy transfer nor chemical reaction dominates, but both play a contributing role in the overall kinetics. The falloff regime spans several orders of magnitude of pressure, and at high temperatures many unimolecular reactions, even at atmospheric pressure, are far from the high-pressure limit. From a practical point of view, rates in the falloff regime are very important, since most CVD processes operate in the 10–760 Torr region.

Reaction rates in the falloff region were calculated at 1300, 1400, and 1500 K for He and H_2 bath gases. Figure 2 shows the dependence of the overall thermal decomposition rate on temperature and pressure over a 10^{-3}–10^{6} Torr pressure range. Based on the calculation discussed in the next section, helium is expected to transfer more energy per collision than hydrogen, which leads to the prediction of slightly higher rates for a helium bath gas at a given temperature and pressure. As can be seen in these plots, only at pressures of about 10^{6} Torr does the rate constant approach its high-pressure limiting value.

Collisional Energy Transfer. In the falloff regime and at the low-pressure limit, the energy distribution of reactant molecules (and thus the reaction rate) depends on the energy transfer occurring in collisions between a reactant molecule and bath gas molecule. To include this effect in the determination of a thermal rate coefficient, one must choose a model for energy transfer and obtain the appropriate values for the energy-transfer parameters. Usually the best strategy is to find experimentally measured values

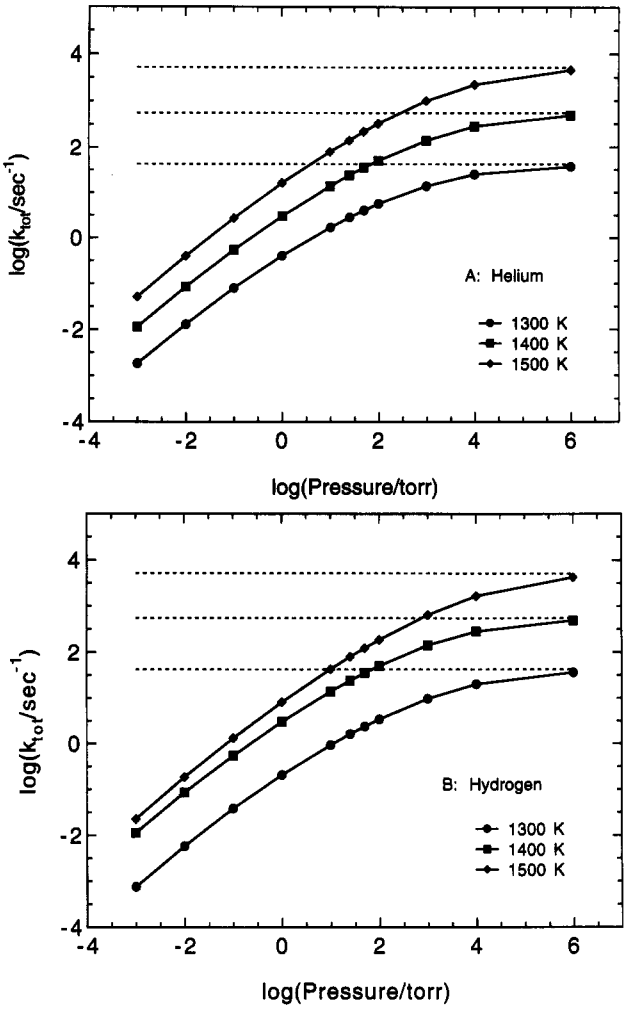

Figure 2. RRKM predictions for the total MTS decomposition rate as a function of temperature and pressure. Dashed lines indicate the high-pressure limit for each temperature. (A) Helium bath gas; (B) hydrogen bath gas.

TABLE 4: Methyltrichlorosilane Collisional Energy-Transfer Parameters from the BRW Model[a]

	He[b]				H_2	
T (K)	S	ΔE_{down}	$^1/_2S$	ΔE_{down}	S	ΔE_{down}
1300	614.5	795.6	307.25	369.8	346.2	420.9
1400	663.1	853.2	331.55	398.2	385.2	468
1500	714.4	913.8	357.2	427.8	422.6	512.5

[a] s and ΔE_{down} in units of cm^{-1}. [b] Collision partner.

of the energy transferred per collision, for either the system of interest or similar systems, and apply the appropriate model.

However, as mentioned earlier, little information is available on collisional energy transfer between chlorinated or alkylated silanes and the bath gases of interest. For this reason we used the semiempirical BRW model for collisional energy transfer.[57-59] This model assumes that, during a collision, energy exchange between the internal degrees of freedom of the excited molecule and the bath gas is essentially random but constrained by microscopic reversibility and total energy conservation. In the BRW model the collisional energy transfer is characterized by the quantity $s = (t_c D_E)^{1/2}$ where t_c is the duration of a collision and D_E is an "energy diffusion coefficient". This model has been tested by comparison with trajectory calculations and incorporates many essential features of the collision dynamics including a temperature dependence. Values of the parameter s calculated for this study are given in Table 4. Equivalent ΔE_{down} (the average downward energy transferred per collision[32] in the exponential-down model) are also reported in Table 4. Since the corresponding ΔE_{down} values for helium are fairly large,[63] we also calculated

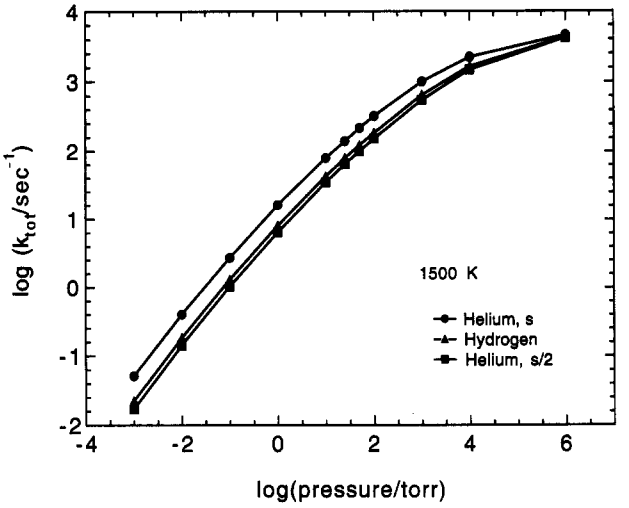

Figure 3. Comparison of RRKM predictions for the total MTS decomposition rate as a function of pressure for different bath gases and amount of energy transferred per collision (as characterized by the parameter s in the BRW model; see text).

rate coefficients with the helium s values divided by two. The $s/2$ value should provide a lower bound for the collisional energy transfer. It should be noted, however, that the calculated values in Table 4 are not unreasonable when compared to values obtained at intermediate temperatures for alkyl isocyanides.[64] In the final analysis, calculations of the overall rates as well as branching fractions are fairly insensitive to the collisional energy-transfer parameter. This is shown in Figure 3, where, at pressures higher than 10 Torr in He, the rates calculated using s and $s/2$ are within about a factor of 2 of each other.

Reaction Branching. Figures 4 and 5 show the results of falloff calculations for the rates of the individual reactions at 1300 and 1500 K, respectively. Comparison of the rates in these two plots shows that the reaction branching has only a minor dependence on the temperature or the collisional energy transfer (based on a comparison of helium and hydrogen bath gases). Although we have not included plots at 1400 K or using $s/2$ for helium, they also support these conclusions. Rate constants for the individual reactions at selected pressures are given in Table 5.

Table 5 and Figures 4 and 5 have several interesting features. First, loss of HCl has the lowest threshold by at least a 1.0 kcal/mol, but because of its relatively tight transition state compared with the bond scissions, it only contributes a small fraction to the overall reaction rate at these temperatures and pressures. Second, with increasing temperature, the rate at a given pressure is further from the high-pressure limit (Table 5). At atmospheric pressure the total rate at 1300 K in a hydrogen bath gas is expected to be about 20% of the high-pressure rate while at 1500 K it is expected to be about 11% of the high-pressure rate. Third, reaction 2 becomes more significant with increasing temperature and pressure, eventually overcoming reaction 4 at pressures between 50 and 100 Torr (1300–1500 K). At atmospheric pressure, reaction 2 is about 4 times faster than reaction 4. A fourth interesting feature is the relatively large contribution of reaction 2 at the higher pressures, even though this channel involves an atom loss reaction that has a threshold at least 5 kcal/mol higher than reaction 1.

The increased importance of reaction 2 arises because its A factor is nearly the same as that for Si–C bond scission (Table 3). The magnitude of the A factor is surprising, since atom-loss reactions involve transition states with only one 2-dimensional internal rotor instead of the two associated with polyatomic leaving groups.[65,66] For bond-cleavage reactions, the 2-dimensional internal rotors usually contribute most of the entropy increase between reactant and transition state. Therefore, one would usually expect an atom-loss transition state to have a *lower* entropy compared to a transition state having two polyatomic frag-

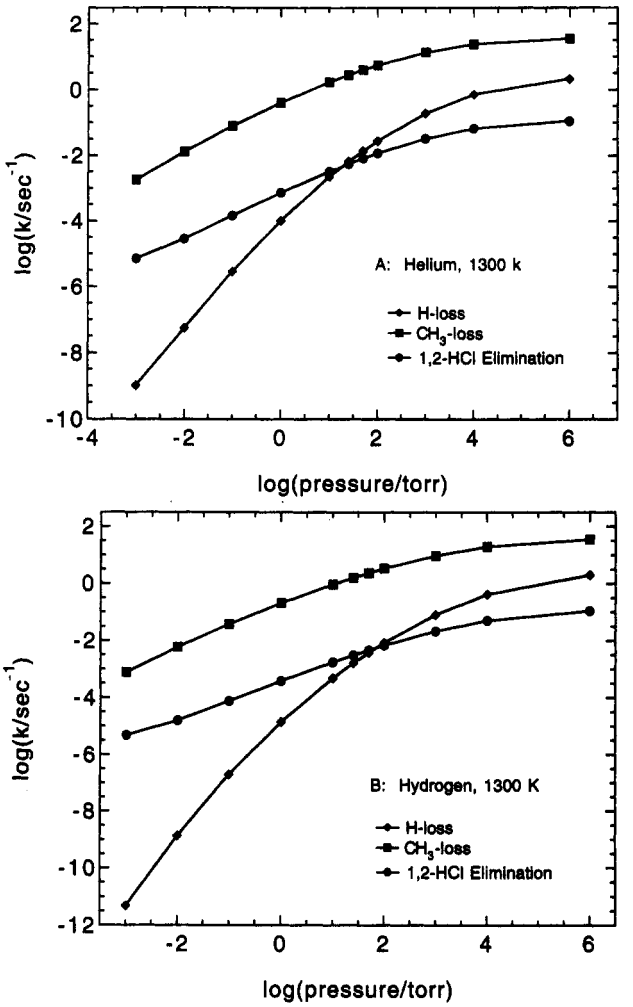

Figure 4. Branching fractions for MTS decomposition as a function of pressure at 1300 K: (A) helium bath gas, (B) hydrogen bath gas.

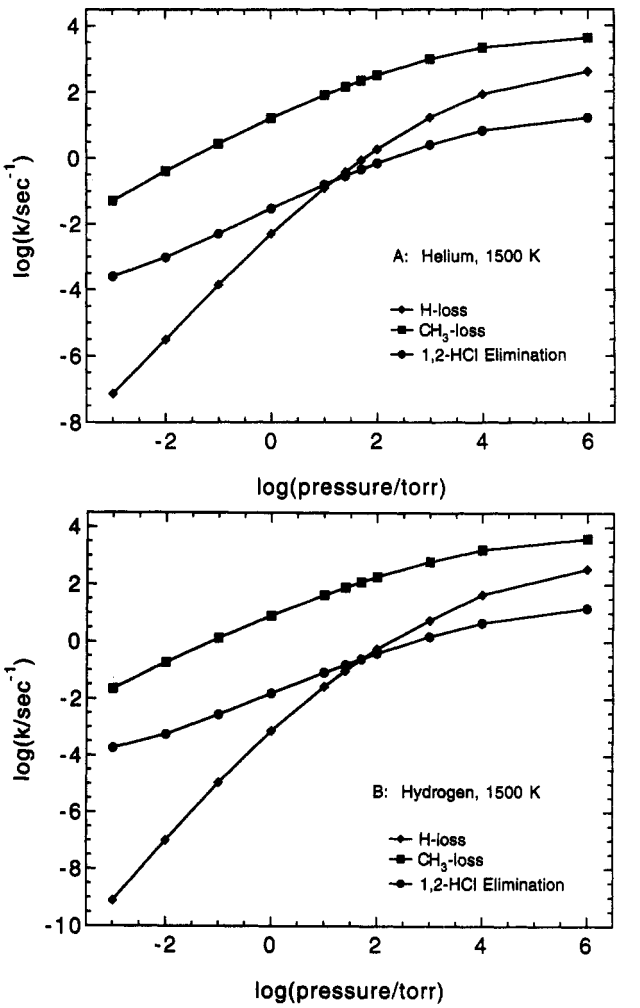

Figure 5. Branching fractions for MTS decomposition as a function of pressure at 1500 K: (A) helium bath gas, (B) hydrogen bath gas.

ments.[65,66] It should be noted that we used a reduced moment of inertia for the 2-dimensional rotor in the transition state of reaction 2 and thus should not have overestimated its entropy contribution.

The surprising A factor for reaction 2 can be understood by considering all of the entropy gains and losses in going from ground-state MTS to the various transition states. Table 6 compares the contributions to the total $\Delta S^{\ddagger}$ for H loss versus CH_3 loss at 1500 K. Although the CH_3 loss transition state has a larger rotational entropy than the transition state for H loss, this comes at a significant cost in vibrational entropy since the Si–C bond has been broken ($\Delta S^{\ddagger}_{vib} = -17.0$ cal mol^{-1} K^{-1}). The low-frequency Si–C vibrations contribute substantially to the entropy of MTS. In contrast, the H-loss transition state has a lower rotational entropy than the CH_3-loss transition state, but the change in vibrational entropy is much less ($\Delta S^{\ddagger}_{vib} = -3.1$ cal mol^{-1} K^{-1}) because the high-frequency C–H vibrations contribute little to the entropy of MTS. The entropy of the H-loss transition state also increases due to the los of molecular symmetry.

To summarize, in the H-loss transition state, loose modes are formed from degrees of freedom that do not contribute much to the entropy of MTS, whereas in the other transition states, the loose modes are formed from degrees of freedom that *do* contribute significantly to the entropy of MTS. Thus, although the rotational entropy is lower for the H-loss transition state, its vibrational entropy is higher.

Sources of Error. As indicated in the Introduction, little experimental or theoretical work has been done on these systems so that a quantitative analysis of the error is not straightforward. However, this section will attempt to provide some indication of the uncertainty. Throughout the discussion of these calculations we have indicated where we had to resort to calculated parameters or simplifications of the dynamic model. In most cases we have attempted to assess the potential for error in our calculations resulting from even gross inaccuracy in a parameter. Most of these assessments are included in the foregoing discussion. Extreme modifications in a given parameter typically changed calculated rate coefficients by less than a factor of 2.

One important input to the calculations whose accuracy we have not discussed so far is the reaction threshold, which was determined from *ab initio* calculations due to the paucity of experimental measurements on these systems. Accuracy estimates of the calculations,[53] which include results from lower level calculations, indicate that the heats of formations of each species are expected to be good to ±2 kcal/mol, particularly for those involved in the bond cleavages.[1,12] The accuracy of the threshold for HCl elimination is less easily determined as it involves a calculation using a transition-state structure. However, the *calculated* error estimate for the heat of formation of this transition state is still within ±2 kcal/mol.[1,12] To assess the importance of changes in reaction thresholds, we calculated rate coefficients with each threshold shifted by ±2 kcal/mol. In the high-pressure limit, shifting a threshold down by 2 kcal/mol causes the rate coefficient to increase by about a factor of 2 for each of the reactions. Correspondingly, shifting a threshold up by 2 kcal/mol causes the rate coefficient to drop by about a factor of 2. The same results were observed for calculations at both 1300 and 1500 K.[67]

To evaluate the magnitude of this effect in the falloff region, we also calculated rate coefficients at 100 Torr. A change of ±2 kcal/mol in a given threshold causes a corresponding increase or decrease in the calculated rate coefficient for that reaction of a

TABLE 5: Rate Coefficients for Reactions of Methyltrichlorosilane

bath gas	T (K)	P (Torr)	k_{HCl} (s^{-1})	k_{CH_3} (s^{-1})	k_H (s^{-1})	k_{tot}/k^{∞}_{uni}
He	1300	10	3.23×10^{-3}	1.71	2.24×10^{-3}	4.07×10^{-2}
		25	5.54×10^{-3}	2.83	6.52×10^{-3}	6.75×10^{-2}
		50	8.15×10^{-3}	4.03	1.38×10^{-2}	9.64×10^{-2}
		100	1.17×10^{-2}	5.60	2.77×10^{-2}	0.134
		760	2.95×10^{-2}	12.5	0.157	0.302
		1000	3.28×10^{-2}	13.7	0.192	0.331
	in low-pressure limit, $k_0 = 4.63 \times 10^8$ cm^3 mol^{-1} s^{-1}					
	1400	10	2.65×10^{-2}	13.8	1.97×10^{-2}	2.5×10^{-2}
		25	4.73×10^{-2}	23.7	5.94×10^{-2}	4.31×10^{-2}
		50	7.2×10^{-2}	34.9	0.13	6.34×10^{-2}
		100	0.107	50.1	0.27	9.12×10^{-2}
		760	0.301	124	1.72	0.228
		1000	0.341	138	2.14	0.253
	in low-pressure limit, $k_0 = 2.72 \times 10^9$ cm^3 mol^{-1} s^{-1}					
	1500	10	0.155	79.4	0.123	1.54×10^{-2}
		25	0.288	142	0.383	2.76×10^{-2}
		50	0.451	215	0.859	4.18×10^{-2}
		100	0.694	318	1.84	6.2×10^{-2}
		760	2.16	863	13.0	0.17
		1000	2.47	970	16.5	0.192
	in low-pressure limit, $k_0 = 1.17 \times 10^{10}$ cm^3 mol^{-1} s^{-1}					
H_2	1300	10	1.73×10^{-3}	0.928	4.8×10^{-4}	2.21×10^{-2}
		25	3.04×10^{-3}	1.6	1.61×10^{-3}	3.81×10^{-2}
		50	4.59×10^{-3}	2.35	3.79×10^{-3}	5.61×10^{-2}
		100	6.78×10^{-3}	3.38	8.43×10^{-3}	8.07×10^{-2}
		760	1.89×10^{-2}	8.51	6.37×10^{-2}	0.204
		1000	2.13×10^{-2}	9.47	8.07×10^{-2}	0.228
	in low-pressure limit, $k_0 = 2.00 \times 10^8$ cm^3 mol^{-1} s^{-1}					
	1400	10	1.41×10^{-2}	7.45	4.29×10^{-2}	1.35×10^{-2}
		25	2.58×10^{-2}	13.3	1.49×10^{-2}	2.41×10^{-2}
		50	4.01×10^{-2}	20.1	3.6×10^{-2}	3.65×10^{-2}
		100	6.11×10^{-2}	29.8	8.23×10^{-2}	5.41×10^{-2}
		760	0.188	81.9	0.685	0.150
		1000	0.215	92.4	0.881	0.169
	in low-pressure limit, $k_0 = 1.22 \times 10^9$ cm^3 mol^{-1} s^{-1}					
	1500	10	8.19×10^{-2}	42.5	2.68×10^{-2}	8.26×10^{-3}
		25	0.155	78.3	9.54×10^{-2}	1.52×10^{-2}
		50	0.247	122	0.236	2.36×10^{-2}
		100	0.388	185	0.553	3.60×10^{-2}
		760	1.3	554	5.04	0.109
		1000	1.51	632	5.67	0.124
	in low-pressure limit, $k_0 = 5.28 \times 10^9$ cm^3 mol^{-1} s^{-1}					

TABLE 6: Entropy Changes between MTS and H Loss or CH_3 Loss Transition States[a,b]

reaction	$\Delta S^{\ddagger}_{vib}$	$\Delta S^{\ddagger}_{rot}$	$\Delta S^{\ddagger}_{sym}$	$\Delta S^{\ddagger}_{tot}$
CH_3	−17.0	+35.0[c]	0	+18.0
H	−3.1	+18.5[c]	+2.2	+17.6

[a] In cal mol^{-1} K^{-1}. [b] At 1500 K. [c] Includes contributions from the external rotations.

factor of about 2–3 at this pressure, except for reaction 2 where the coefficient changes by a factor of 4–5. Shifting the threshold for HCl elimination has essentially no effect on the rate coefficients for the other reactions because it has such a minor contribution to the overall decomposition. Shifting the threshold for the H-loss reaction also has little effect on the calculated rate coefficients for the other reactions. This is not surprising because the reaction has a higher threshold and because its contribution is significant only at pressures well above 100 Torr. Shifting the CH_3 loss threshold, however, has a substantial effect on the other reactions. Decreasing this threshold by 2 kcal/mol decreases the rate coefficient for HCl loss by about a factor of 2, while the rate coefficient for H loss decreases by a factor of 3–4. A threshold 2 kcal/mol higher causes a 50% increase in the rate of HCl elimination and a factor of 2–3 increase in the rate of H loss. Results consistent with these conclusions were observed for calculations at both 1300 and 1500 K using bath gases of helium or hydrogen.

Thus, in the falloff regime, the overall rate is most sensitive to the threshold for reaction 1, as is expected.[52] Of the three channels, thermodynamic data for the products of reaction 1 should be the most accurate since CH_3 is well characterized and $SiCl_3$ has fewer empirical corrections[12] required to obtain its heat of formation than CH_2SiCl_3. Of course, its relative threshold will still depend on the thermodynamic data for the other reactions. In the next section, we will also show that our calculations are in good agreement with a measured association rate for CH_3 and $SiCl_3$.

Comparison to Experimental Association Rate. Niiranen and Gutman recently investigated the association rate for CH_3 and $SiCl_3$ (reverse of reaction 1) in the high-pressure limit.[50] They report an association rate of 1.1×10^{-10} cm^3 molecule^{-1} s^{-1} at 303 K.[50] At the same temperature and pressure,[68] we calculate a *dissociation* rate of 9.2×10^{-53} s^{-1} using the canonical variational transition-state theory treatment.[69] The association rate and dissociation rate are related by the equilibrium constant (eq 7).[13] Using thermodynamic data from earlier BAC-MP4 calculations,[12] we evaluated the equilibrium constant and obtained $K_{eq} = 3.9 \times 10^{-43}$ molecule cm^{-3}. Equation 7 then yields an association rate of 2.4×10^{-10} cm^3 molecule^{-1} s^{-1} based on the calculated dissociation rate. This agrees reasonably well with the experimentally measured association rate.[70]

$$K_{eq} = k^{\infty}_{uni}/k^{\infty}_{assoc} \tag{7}$$

Discussion

Significance for Organosilicon Chemistry. We have provided quantitative estimates for what are predicted to be the three most important unimolecular reactions of methyltrichlorosilane, a compound whose decomposition is of intense interest. As discussed in the Introduction, experimental and theoretical treatments of the chlorinated organosilanes are nearly nonexistent. The results of this study thus provide new insight into the characteristic features of chlorinated organosilicon chemistry, in particular the ways in which reactions of these molecules differ from those of species containing no chlorine and from analogous hydrocarbon chemistry.

Our results highlight three factors that have an important influence on the reactions of chlorinated organosilanes. The first is the high strength of the Si–Cl bond, which in MTS[12] is 114 kcal mol^{-1} vs 92 kcal mol^{-1} for the Si–H bond in CH_3SiH_3.[1] The effect of this large bond dissociation energy is to make pathways that do not involve breaking the bond, such as CH_3 loss and H loss, energetically favorably. At the same time, the Si–Cl bond strength contributes to higher reaction thresholds requiring higher temperatures to observe significant decomposition. In addition, the presence of these strong bonds undoubtedly reduces the rates of silylene elimination reactions (for example, reactions 5 and 6), although the magnitude of this effect is difficult to evaluate relative to the reduction in rate caused by the increased electronegativity of chlorine.[71] As discussed earlier, silylene eliminations in MTS (reactions 5 and 6, see Figure 1) are relatively high-energy pathways for decomposition.

Second, the 1,2-elimination pathway in MTS (96.9 kcal mol^{-1} at 1400 K in the high-pressure limit) is energetically accessible; its activation barrier is actually lower than the barriers for H loss and CH_3 loss (103.8 and 97.5 kcal mol^{-1} at 1400 K in the high-pressure limit). This contrasts with the situation in CH_3SiH_3, where the corresponding reaction, 1,2-elimination of H_2, is much higher than other reaction pathways.[7] The relatively low reaction threshold for the 1,2-elimination arises from the ionic character of the transition state and is thus another consequence of the Cl functionality.[15,16]

The third important factor is the formation of product fragments with large moments of inertia, which leads to large A factors and,

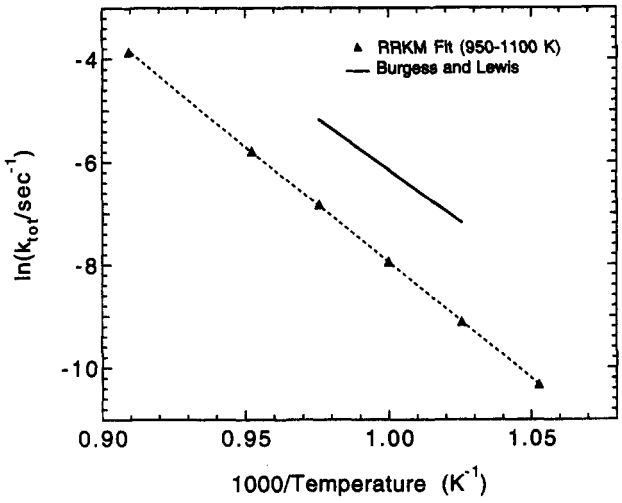

Figure 6. Comparison of experimental results of Burgess and Lewis (ref 25) with RRKM predictions of the total MTS decomposition rate at 760 Torr in hydrogen. Triangles indicate temperatures at which the RRKM calculations were performed; the dashed line is a linear least-squares fit of the Arrhenius rate expression to these points.

hence, higher reaction rates. In the case of MTS, this is illustrated by the CH_3-loss reaction (reaction 4), with a high-pressure A factor at 1300 K that is predicted to be 10^{18} s^{-1}. This can be compared with the analogous reaction for CH_3CH_3, where the high-pressure A factor[72] is 2×10^{17} s^{-1}. Presumably, high A factors will also be observed in other chlorinated organosilanes. Steric factors may, however, reverse (or at least mitigate) this trend; the bulkiness of groups such as $SiCl_3$ relative to SiH_3 may tighten the transition state, thus lowering the transition-state entropy.

The factors discussed above combine to make bond-scission pathways the most efficient ones for MTS unimolecular decomposition. In particular, the dominant reaction is Si–C bond cleavage. This indicates that intuition based on the reactivity of organosilanes that do not contain Si–Cl bonds cannot be straighforwardly extended to chlorinated species, since silylene elimination reactions are usually the lowest-energy channels for simple organosilanes (especially for compounds containing at least one Si–H bond) and 1,2-eliminations are usually much higher in energy. These characteristics of chlorinated organosilanes lead to the possibility that radical chain processes may occur during the pyrolysis of chlorinated organosilanes, which can complicate experimental measurements of decomposition rates. Mechanisms of this type have been observed for the decomposition of several methylchlorosilanes,[10] although MTS was not among them.

Implications for SiC CVD. The results of this study have several important implications for understanding SiC CVD processes that use MTS as a reactant. First, the experimental reaction rates of BL,[25] which have been widely used in modeling SiC CVD, are substantially higher than those predicted by the RRKM calculations. Figure 6 shows a comparison of the total MTS decomposition rate as determined by BL at a pressure of 760 Torr in hydrogen, compared with the RRKM results for the same conditions. The MTS decomposition rate predicted by RRKM ($k_{tot}(H_2,760\,Torr) = 1.4 \times 10^{16} \exp(-89650/RT)$ (s^{-1}), $T = 950$–1100 K) is a factor of 5–7 smaller than the experimental result ($k_{tot}(H_2,1\,atm) = 7.6 \times 10^{14} \exp(-80300/RT)$ (s^{-1}), $T = 975$–1025 K). Our evaluation of the uncertainties associated with the RRKM calculations indicates that the rate reported in the BL paper is outside the estimated error of the calculations. In particular, transition-state theory is inherently expected to overestimate reaction rates because it does not account for barrier recrossing.[32] Barring a gross inaccuracy in a reaction threshold (unlikely, *vide supra*), our calculations would be expected to *overestimate* the decomposition rate. The reasons for this discrepancy are unclear; radical chain processes are a possibility, especially since BL's measurements were made at relatively low temperatures. Unfortunately, the BL paper only reports an Arrhenius expression and no data or error analysis, making a critical comparison difficult. Ironically, extrapolation of the BL results to typical SiC CVD temperatures (1300–1500 K) brings them into closer agreement with the RRKM results (about a factor of 3 larger than the RRKM results for an H_2 bath gas). Further experimental measurements are required to resolve this discrepancy. On the basis of our evaluation of the uncertainties in the RRKM rate constants, we conclude that these rates are more likely to represent the true unimolecular MTS decomposition rate than the BL experimental result, which was obtained from a complex system in which a large number of reactions may have been occurring.

A second point relevant to SiC CVD is that pressure effects on the decomposition rate of MTS are large. For example, at atmospheric pressure and 1400 K, k/k_∞ is 0.15, while at 25 Torr, k/k_∞ is 0.024. Thus, accurate simulations of SiC CVD processes must take into account the pressure falloff of the reactant pyrolysis reactions. In particular, it should be noted that the results of BL should not be extended to low pressures.

From a mechanistic standpoint, the RRKM results show that at atmospheric pressure the predominant decomposition mode is expected to be loss of CH_3. In the presence of hydrogen carrier gas, CH_3 will lead to the production of large quantities of methane. The $SiCl_3$ radical that is formed can undergo unimolecular decomposition to form $SiCl_2$ and Cl ($\Delta H°_{rxn}(298\,K) = 68.8$ kcal mol^{-1}) or react exothermically with CH_3 to form CH_3Cl and $SiCl_2$ ($\Delta H°_{rxn}(298\,K) = -15.0$ kcal mol^{-1}) or react with H_2 to form $SiCl_3H$ and H ($\Delta H°_{rxn}(298\,K) = 10.9$ kcal mol^{-1}). Thus, the gas-phase species in highest concentration during deposition may be $SiCl_2$, CH_4, and $SiCl_3H$. The reactivity of $SiCl_2$ at high temperatures is uncharacterized, pointing again to the need for additional experimentation.

Organosilicon species may play a role in the deposition of SiC, especially if they are radicals. The surface reactivity of organosilicon radicals should be much greater than that of methane, which is likely to be the most abundant hydrocarbon present in the gas phase and whose reactive sticking coefficient is probably[73] 10^{-5}–10^{-4}. Our results show that two organosilicon radicals[74] are formed by the initial decomposition of MTS, $Cl_2Si{=}CH_2$ and CH_2SiCl_3. The latter species, assuming that its reactivity is similar to methane, will be rapidly reconverted to MTS via reaction with the hydrogen carrier gas. Use of inert carrier gas or high MTS partial pressures favors relatively higher concentrations of this molecule, however. The remaining radical, the silaethylene $Cl_2Si{=}CH_2$, represents <0.4% of the products at all pressures examined. The surface reactivity of this molecule is unknown; if it is similar to C_2H_4 ($\Gamma \sim 0.001$ on silicon surfaces[73]), it could contribute significantly to the deposition of carbon. Thus, the calculations reported here indicate that pathways are available for the production of organosilicon radicals with potentially high surface reactivity. Their concentrations relative to CH_4 must first be known, however, to determine their importance to the deposition process.

Finally, the effect of substituting an inert carrier gas such as helium for hydrogen in a SiC CVD process can be evaluated from the RRKM results. The data shown in Figure 2 indicate that the rates of reactions 1 and 4 increase by about a factor of 2 or less when the carrier gas is helium instead of hydrogen. The rate of reaction 2 increases more, about a factor of 6.5 at 25 Torr. Such effects are relatively small, however, compared with the change induced by the substitution of a reactive gas such as hydrogen for an unreactive one such as helium. Thus, a different gas-phase product distribution is expected from the two carrier gases, which could alter the SiC deposition rate substantially.

Conclusions

Using RRKM theory, we calculated rate constants for the decomposition of MTS in both the high-pressure limit and in the

falloff regime. The results show that Si–C bond cleavage, C–H bond cleavage, and HCl elimination (reactions 1, 2, and 4) are the predominant thermal decomposition pathways. Reaction 1 is the most efficient decomposition pathway at the temperatures of interest. However, at atmospheric pressure, reaction 2 and reaction 4 have minor contributions as well. As the pressure decreases, the rate of reaction 2 decreases substantially.

The relative importance of the H atom loss channel (reaction 2) is surprising. The large A factor for this reaction is due to the relatively minor loss of vibrational entropy from breaking a C–H bond instead of C–(heavy atom) bond. This makes up for the lower entropy contribution of only one 2-dimensional rotor in the C–H bond cleavage transition state. We also point out that, in contrast to other organosilanes, this reaction is thermodynamically accessible because the strong Si–Cl bonds in MTS raise the activation barriers for reactions that are normally considerably lower than that for H loss. Similarly, the presence of chlorine atoms lowers the threshold for the 1,2-elimination because of contributions from orbitals having ionic character.[15,16]

Prior to this work, little information was available on the gas-phase kinetic behavior of chlorinated organosilanes even though they are an important class of compounds in many fields. The results reported here provide new insight into the decomposition reactions of these compounds as well as quantitative estimates of their rates. A calculated association rate at room temperature is compared to a recent experimental measurement and found to be in good agreement. The behavior of these systems is predicted to be very different from the nonchlorinated organosilicon analogs. Along with mechanistic discussions,[10] the present study provides a critically needed starting point for future theoretical and experimental investigations of the reactivity of these systems.

Acknowledgment. This work was supported by the U.S. Department of Energy, Office of Industrial Technologies, Advanced Industrial Materials Program. We thank Professor John Brauman as well as Dr. Brian Wladkowski, Dr. Sean Smith, and Dr. Kieran Lim for insights and helpful discussion.

References and Notes

(1) Allendorf, M. D.; Melius, C. F. *J. Phys. Chem.* **1992**, *96*, 428.
(2) Walsh, R. In *The Chemistry of Organic Silicon Compounds*; Patai, S., Rappoport, Z., Eds.; John Wiley and Sons: New York, 1989; pp 371–391.
(3) Safarik, I.; Sandhu, V.; Lown, E. M.; Strausz, O. P.; Bell, T. N. *Res. Chem. Intermed.* **1990**, *14*, 105–131.
(4) Gaspar, P. P. In *Reactive Intermediates*; Jones Jr., M., Moss, R. A., Eds.; Wiley: New York, 1985; Vol. 3, pp 333–427.
(5) Tang, Y.-N. In *Reactive Intermediates*; Abramovitch, R. A., Ed.; Plenum: New York, 1982; Vol. 2, pp 297–367.
(6) Gordon, M. S.; Gano, D. R. *J. Am. Chem. Soc.* **1984**, *106*, 5421.
(7) Gordon, M. S.; Truong, T. N. *Chem. Phys. Lett.* **1987**, *142*, 110.
(8) Neudorfl, P. S.; Lown, E. M.; Safarik, I.; Jodhan, A.; Strausz, O. P. *J. Am. Chem. Soc.* **1987**, *109*, 5780.
(9) Sawrey, B. A.; O'Neal, H. E.; Ring, M. A.; Coffey, Jr., D. *Int. J. Chem. Kinet.* **1984**, *16*, 31.
(10) Davidson, I. M. T.; Dean, C. E. *Organometallics* **1987**, *6*, 966.
(11) Su, M.-D.; Schlegel, H. B. *J. Phys. Chem.* **1993**, *97*, 9981.
(12) Allendorf, M. D.; Melius, C. F. *J. Phys. Chem.* **1993**, *97*, 720.
(13) Benson, S. W. *Thermochemical Kinetics*, 2nd ed.; J. Wiley and Sons: New York, 1976.
(14) McMillen, D. F.; Golden, D. M. *Annu. Rev. Phys. Chem.* **1982**, *33*, 493.
(15) Maccoll, A. In *The Chemistry of Alkenes*, 1st ed.; Patai, S., Ed.; Interscience Publishers: New York, 1964; Vol. 1, pp 203–240.
(16) Maccoll, A. In *Advances in Physical Organic Chemistry*; Gold, V., Ed.; Academic Press: New York, 1965; Vol. 3, pp 91–122.
(17) Voorhoeve, R. J. H. *Organohalosilanes: Precursors to Silicones*; Elsevier: New York, 1967.
(18) Besmann, T. M.; Sheldon, B. W.; Lowden, R. A.; Stinton, D. P. *Science* **1991**, *253*, 1104.
(19) Besmann, T. M.; Sheldon, B. W.; Kaster, M. D. *Surface Coatings Technol.* **1990**, *43/44*, 167.
(20) Motojima, S.; Hasegawa, M. *J. Vac. Sci. Technol. A* **1990**, *8*, 3763.
(21) Cheng, D. J.; Shyy, W. J.; Kuo, D. H.; Hon, M. H. *J. Electrochem. Soc.* **1987**, *134*, 3145.
(22) Kuo, D. H.; Cheng, D. J.; Shyy, W. J.; Hon, M. H. *J. Electrochem. Soc.* **1990**, *137*, 3688.
(23) So, M. G.; Chun, J. S. *J. Vac. Sci. Technol. A* **1988**, *6*, 5.
(24) Yeheskel, J.; Agam, S.; Dariel, M. S. *Chemical Vapor Deposition 1990*; Spear, K. E., Cullen, G. W., Eds.; The Electrochemical Society Softbound Proceedings Series: Seattle, 1990.
(25) Burgess, J. N.; Lewis, T. J. *Chem. Ind.* **1974**, 76.
(26) Whitman, L. J.; Joyce, S. A.; Yarmoff, J. A.; Mcfeely, F. R.; Terminello, L. J. *Surf. Sci.* **1990**, *232*, 297.
(27) NoorBatcha, I.; Raff, L. M.; Thompson, D. L. *J. Chem. Phys.* **1984**, *81*, 3715.
(28) Ho, P.; Breiland, W. G.; Buss, R. J. *J. Chem. Phys.* **1989**, *91*, 2627.
(29) Robertson, R. M.; Rossi, M. J. *Appl. Phys. Lett.* **1989**, *54*, 185.
(30) Perrin, J.; Broekhuizen, T. *Appl. Phys. Lett.* **1987**, *50*, 433.
(31) Gardiner, Jr., W. C.; Troe, J. In *Combustion Chemistry*; Gardiner Jr., W. C., Ed.; Springer-Verlag: New York, 1984, pp 173–196.
(32) Gilbert, R. G.; Smith, S. C. *Theory of Unimolecular and Recombination Reactions*; Blackwell Scientific Publications: Oxford, 1990.
(33) Jordan, M. J. T.; Smith, S. C.; Gilbert, R. G. *J. Phys. Chem.* **1991**, *95*, 8685.
(34) Pitt, I. G.; Gilbert, R. G.; Ryan, K. R. *Aust. J. Chem.* **1990**, *43*, 169.
(35) Greenhill, P. G.; Gilbert, R. G. *J. Phys. Chem.* **1986**, *90*, 3104.
(36) Berne, B. J.; Borkovec, M.; Straub, J. E. *J. Phys. Chem.* **1988**, *92*, 3711.
(37) Forst, W. *Theory of Unimolecular Reactions*; Academic Press: New York, 1973.
(38) Karas, A. J.; Gilbert, R. G. *J. Phys. Chem.* **1992**, *96*, 10893.
(39) Klippenstein, S. J.; Marcus, R. A. *J. Chem. Phys.* **1989**, *91*, 2280.
(40) Klippenstein, S. J. *J. Chem. Phys.* **1990**, *93*, 2418.
(41) Klippenstein, S. J. *J. Chem. Phys.* **1991**, *94*, 6469.
(42) Marcus, R. A. *Science* **1992**, *256*, 1523.
(43) Miller, W. H. *J. Chem. Phys.* **1976**, *65*, 2216.
(44) Ravi, R.; Takoudis, C. G. *J. Electrochem. Soc.* **1992**, *139*, 1994.
(45) Robinson, P. J.; Holbrook, K. A. *Unimolecular Reactions*; John Wiley and Sons: New York, 1972.
(46) Smith, S. C.; Gilbert, R. G. *Int. J. Chem. Kinet.* **1988**, *20*, 307.
(47) Troe, J. *J. Chem. Phys.* **1977**, *66*, 4745.
(48) Troe, J. *J. Chem. Phys.* **1977**, *66*, 4758.
(49) Wardlaw, D. M.; Marcus, R. A. *Adv. Chem. Phys.* **1987**, *70*, 231.
(50) Niiranen, J. T.; Gutman, D. *J. Phys. Chem.* **1993**, *97*, 9392.
(51) Gilbert, R. G.; Jordan, M. J. T.; Smith, S. C. UNIMOL program suite, 1992.
(52) Allendorf, M. D.; Melius, C. F.; Osterheld, T. H. In *Chemical Vapor Deposition 1993 Softbound Proceedings Series*; Cullen, G. W., Jenson, K., Eds.; The Electrochemical Society: Pennington, NJ, 1993, in press.
(53) Ho, P.; Melius, C. F. *J. Phys. Chem.* **1990**, *94*, 5120.
(54) Soliman, M. S.; Khattab, M. A.; El-Kourashy, A. G. *Spectrochim. Acta* **1983**, *39A*, 621.
(55) Chase, M. W. J.; Davies, C. A.; Downey, J. R. J.; Frurip, D. J.; McDonald, R. A.; Syverud, A. N. *J. Phys. Chem. Ref. Data* **1985**, *14*, 860.
(56) Hehre, W. J.; Radom, L.; Schleyer, P. v. R.; Pople, J. A. *Ab Initio Molecular Orbital Theory*; Wiley: New York, 1986.
(57) Gilbert, R. G. *J. Chem. Phys.* **1984**, *80*, 5501.
(58) Lim, K. F.; Gilbert, R. G. *J. Chem. Phys.* **1986**, *84*, 6129.
(59) Lim, K. F.; Gilbert, R. G. *J. Chem. Phys.* **1990**, *92*, 1819.
(60) A 2-dimensional methyl rotor has $\sigma = 2$ because two faces of the planar methyl moiety can be presented to the $SiCl_3$ group. Of course the 1-dimensional methyl rotor has $\sigma = 3$.
(61) $I_r = I_1 I_2/(I_1 + I_2)$.
(62) Melius, C. F. Personal communication.
(63) Both the BRW model and trajectory calculations can overestimate energy-transfer values for collisions with He. For a discussion see refs 32 and 57–59.
(64) Quack, M.; Troe, J. In *A Specialist Periodical Report. Gas Kinetics and Energy Transfer*; Ashmore, P. G., Donovan, R. J., Eds.; The Chemical Society: London, 1977; Vol. 2.
(65) Wladkowski, B. D.; Wilbur, J. L.; Brauman, J. I. *J. Am. Chem. Soc.* **1992**, *114*, 9706.
(66) Wilbur, J. L.; Wladkowski, B. D.; Brauman, J. I. *J. Am. Chem. Soc.* **1993**, *115*, 10823.
(67) The ratio describing the change in the calculated rate resulting from a different reaction threshold is simply $\exp[(E_1 - E_2)/RT]$. This ratio is essentially 2 in all cases since E_1 is nominally 100 kcal/mol for all of the reactions considered and the temperature increase from 1300 to 1500 K is relatively minor.
(68) Our calculations indicate that, under the pressure used for the experiments reported in ref 50, reaction –1 is slightly below the high-pressure limit (by a factor of 0.92). Niiranen and Gutman did not measure the pressure dependence of reaction –1, and it would not be surprising if its high-pressure limit differed slightly from the comparison reactions in which the pressure dependence was measured.
(69) B_{ext}(inact) = 0.025 24 cm^{-1} and average hindrance $\Theta = 80°$.
(70) The fact that this rate is larger than the experimentally measured rate is consistent with the general expectation that a transition-state theory calculation will overestimate rates.
(71) Sosa, C.; Schlegel, H. B. *J. Am. Chem. Soc.* **1984**, *106*, 5847.
(72) Stewart, P. H.; Larson, C. W.; Golden, D. M. *Combust. Flame* **1989**, *75*, 25.
(73) Stinespring, C. D.; Wormhoudt, J. C. *J. Appl. Phys.* **1989**, *65*, 1733.
(74) In this paper we use the term "radical" to refer to any unsaturated species.